HHS Public Access

Author manuscript

Clin Cancer Res. Author manuscript; available in PMC 2017 March 15.

Published in final edited form as:

Clin Cancer Res. 2016 September 15; 22(18): 4623–4633. doi:10.1158/1078-0432.CCR-16-0637.

Comprehensive molecular characterization of salivary duct carcinoma reveals actionable targets and similarity to apocrine breast cancer

Martin G. Dalin[1], **Alexis Desrichard**[1], **Nora Katabi**[2], **Vladimir Makarov**[1], **Logan A. Walsh**[1], **Ken-Wing Lee**[1], **Qingguo Wang**[1], **Joshua Armenia**[1], **Lyndsay West**[3], **Snjezana Dogan**[2], **Lu Wang**[2], **Deepa Ramaswami**[1], **Alan L. Ho**[4], **Ian Ganly**[1,3], **David B. Solit**[1,5,6], **Michael F. Berger**[2,5], **Nikolaus D. Schultz**[7], **Jorge S. Reis-Filho**[1,2], **Timothy A. Chan**[*,1,8], and **Luc G.T. Morris**[*,1,3]

[1]Human Oncology and Pathogenesis Program, Memorial Sloan Kettering Cancer Center, New York, NY, USA

[2]Department of Pathology, Memorial Sloan Kettering Cancer Center, New York, NY, USA

[3]Department of Surgery, Memorial Sloan Kettering Cancer Center, New York, NY, USA

[4]Head and Neck Medical Oncology Service, Department of Medicine, Memorial Sloan Kettering Cancer Center, New York, NY

[5]Marie-Josée and Henry R. Kravis Center for Molecular Oncology, Memorial Sloan Kettering Cancer Center, New York, New York, USA

[6]Genitourinary Oncology Service, Department of Medicine, Memorial Sloan Kettering Cancer Center, New York, New York, USA

[7]Department of Epidemiology and Biostatistics, Memorial Sloan Kettering Cancer Center, New York, NY, USA

[8]Department of Radiation Oncology, Memorial Sloan Kettering Cancer Center, New York, NY, USA

[*]Corresponding authors: Timothy A. Chan, 1275 York Avenue, Box 20, Memorial Sloan Kettering Cancer Center, New York, NY 10065. Phone: 646-888-2765; Fax: 646-8882595; chant@mskcc.org Luc G.T. Morris, Memorial Sloan Kettering Cancer Center, 1275 York Avenue, New York, NY 10065. Phone: 212-639-3049; Fax: 212-717-3278; morrisl@mskcc.org.

Conflict of interest:
The authors declare no conflict of interest.

Author contributions

- Conception and design (MD, LGTM)
- Development of methodology (MD, AD, VM, JSR-F, TAC, LGTM)
- Acquisition of data (MD, NK, LWe, MFB, DBS, JSR-F, LGTM)
- Analysis and interpretation of data (MD, AD, NK, VM, LAW, QW, JA, NDS, JSR-F, TAC, L-GTM)
- Writing, review and/or revision of the manuscript (MD, JSR-F, TAC, LGTM)
- Administrative, technical, or material support (KWL, LWa, SD, DR, ALH, IG)
- Study supervision (TAC, LGTM)

Abstract

Purpose—Salivary duct carcinoma (SDC) is an aggressive salivary malignancy which is resistant to chemotherapy and has high mortality rates. We investigated the molecular landscape of SDC, focusing on genetic alterations and gene expression profiles.

Experimental Design—We performed whole-exome sequencing, RNA sequencing and immunohistochemical analyses in 16 SDC tumors, and examined selected alterations via targeted sequencing of 410 genes in a second cohort of 15 SDCs.

Results—SDCs harbored a higher mutational burden than many other salivary carcinomas (1.7 mutations/megabase). The most frequent genetic alterations were mutations in *TP53* (55%), *HRAS* (23%), *PIK3CA* (23%), and amplification of *ERBB2* (35%). Most (74%) tumors had alterations in either MAP kinase (*BRAF*/*HRAS*/*NF1*) genes or *ERBB2*. Potentially targetable alterations based on supportive clinical evidence were present in 61% of tumors. Androgen receptor (AR) was overexpressed in 75%; several potential resistance mechanisms to androgen deprivation therapy (ADT) were identified, including the AR-V7 splice variant (present in 50%, often at low ratios compared to full length AR) and *FOXA1* mutations (10%). Consensus clustering and pathway analyses in transcriptome data revealed striking similarities between SDC and molecular apocrine breast cancer.

Conclusions—This study illuminates the landscape of genetic alterations and gene expression programs in SDC, identifying numerous molecular targets and potential determinants of response to AR antagonism. This has relevance for emerging clinical studies of ADT and other targeted therapies in SDC. The similarities between SDC and apocrine breast cancer indicate that clinical data in breast cancer may generate useful hypotheses for SDC.

Keywords

Salivary duct carcinoma; whole exome sequencing; RNA sequencing; mutations; molecular apocrine breast cancer

Introduction

Salivary duct carcinoma (SDC) is one of the most aggressive head and neck tumors, accounting for 2% of salivary gland cancers. The majority of cases originate in the parotid or submandibular gland, with lymph node metastasis and facial nerve palsy common at diagnosis (1, 2). Standard treatment includes surgical resection with or without adjuvant radiotherapy, but local disease recurrence and distant metastasis are common and rarely responsive to chemotherapy. Therefore, the overall prognosis remains poor with a long-term survival of 30–55% (1–3).

SDCs may arise de novo or develop as the malignant component of a carcinoma ex pleomorphic adenoma (denoted SDC ex-PA), which is a cancer that has transformed from a longstanding pleomorphic adenoma. Histological findings include a hyalinized, fibrous stroma infiltrated by neoplastic ducts, which resembles the morphology of invasive ductal carcinoma of the breast (4). SDC and breast cancer also share several immunohistochemistry (IHC) characteristics including positive staining for the androgen receptor (AR), which is

detected in a majority of both tumor types (3, 5–7). Several case series have reported clinical benefit from androgen-deprivation therapy (ADT), which has been suggested as potential first-line therapy in patients with recurrent AR-positive SDC (8, 9).

Amplification of *ERBB2* (also known as human epidermal growth factor receptor 2, *HER2*) has been detected in approximately one-third of SDCs, and is associated with poor prognosis (3, 5, 10, 11). The ERBB2 inhibitor trastuzumab has been tested with reported cases of clinical response (12–14), although no controlled study has been performed. It has been proposed that SDC, analogous to breast cancer, can be divided into different subtypes based on receptor status: AR-positive, ERBB2-positive, and basal-like (AR- and ERBB2-negative) phenotypes (6). However, this hypothesis is based on immunohistochemical data only, and it is unclear whether SDC resembles breast cancer on a broader molecular level.

Previous genetic studies of SDC have focused on a limited number of genes, and have found *TP53* alterations in the majority of patients. Other recurrently mutated genes include *KIT*, *PIK3CA* and *HRAS* (5, 15). To date, no unbiased comprehensive molecular characterization of SDC with whole exome or transcriptome sequencing has been reported.

In this study, we performed whole exome sequencing of tumor and matched normal DNA as well as tumor RNA sequencing, and analyzed the spectrum of genetic alterations in 16 SDC patients. In order to classify SDC in comparison to breast cancer, global gene expression was analyzed and compared to published datasets of breast carcinoma. For additional comparison, we also analyzed targeted sequencing data in a second cohort of 15 recurrent/metastatic SDCs that were profiled as part of an institutional precision medicine platform. We report a high frequency of potentially actionable genetic alterations in this rare, often lethal cancer. Taken together, this is the first comprehensive genetic study of SDC, providing a molecular foundation for future research and clinical trials.

Materials and methods

Case selection

With written informed consent and following Institutional Review Board (IRB) approval, tumor and matched normal (peripheral blood or non-neoplastic normal tissue) specimens were obtained from SDC patients treated at Memorial Sloan Kettering Cancer Center during the years 2000 to 2015. For cohort 1 (denoted SDC1-SDC16), tissue samples were snap frozen in liquid nitrogen at the time of surgery and stored at −80 °C. Hematoxylin and eosin stained tumor sections were independently re-evaluated by a head and neck pathologist (N.K.) confirming the SDC diagnosis. Sixteen cases with sufficient tumor material were subjected to whole exome sequencing of tumor and normal DNA as well as tumor RNA sequencing.

For cohort 2 (denoted SDC17-SDC31), tumors were sequenced using a clinical next-generation sequencing platform, Memorial Sloan Kettering-Integrated Mutation Profiling of Actionable Cancer Targets (MSK-IMPACT) (16). These were patients with advanced (all recurrent or metastatic) cancers who were offered targeted tumor sequencing in the context of an IRB-approved study (NCT01775072). For these cases, tumor DNA and matched

normal blood DNA were subjected to massively parallel sequencing targeting the exons of 410 selected genes and selected intronic and regulatory regions (listed in Supplementary Table 1), with technical details of this assay previously described (16).

DNA and RNA extraction

DNA was extracted from fresh frozen tissue or whole blood using the DNeasy Blood and Tissue Kit (Qiagen), and quantified with the PicoGreen assay (Thermo Fisher Scientific). RNA was extracted using the RNeasy Mini kit (Qiagen), and quantified with the RiboGreen assay (Thermo Fisher Scientific). DNA and RNA quality and integrity was analyzed by BioAnalyzer (Agilent Technologies) and Fragment Analyzer (Advanced Analytics).

Whole exome library preparation and sequencing

Whole exome sequencing libraries were prepared using the SureSelect XT library preparation kit (Agilent). DNA was sheared using a LE220 Focus Ultra-sonicator (Covaris), and the fragments were end-repaired, adenylated, ligated to Illumina sequencing adapters, and amplified by PCR. Exome capture was performed using the SureSelect XT v4 51Mb capture probe set (Agilent) and captured exome libraries were enriched by PCR. Final libraries were quantified using the KAPA Library Quantification Kit (KAPA Biosystems), Qubit Fluorometer (Life Technologies) and 2100 BioAnalyzer (Agilent), and were sequenced on a HiSeq2500 sequencer (Illumina) using 2 x 125bp cycles.

RNA library preparation and sequencing

RNA sequencing libraries were prepared using the KAPA Stranded RNA-Seq with RiboErase sample preparation kit (KAPA Biosystems). Total RNA (100ng) was ribosomal RNA-depleted and fragmented, followed by first and second strand synthesis, A tailing, adapter ligation and PCR amplification (using 11 cycles). Final libraries were quantified using the KAPA Library Quantification Kit (KAPA Biosystems), Qubit Fluorometer (Life Technologies) and 2100 BioAnalyzer (Agilent), and were sequenced on a HiSeq2500 v4 chemistry sequencer (Illumina) using 2 x 125bp cycles.

Mutation analysis

The match between tumor and normal samples of each patient was confirmed with fingerprinting analysis using an in-house panel of 118 single nucleotide-polymorphisms, and with VerifyBamID (17). Raw sequencing data were aligned to the hg19 genome build using the Burrows-Wheeler Aligner (BWA) version 0.7.10 (18). Indel realignment, base quality score recalibration and removal of duplicate reads were performed using the Genome Analysis Toolkit (GATK) version 3.2.2 (broadinstitute.org/gatk), following guidelines for raw read alignment (19).

Single nucleotide variations (SNVs) were independently detected by 4 callers; MuTect (broadinstitute.org/cancer/cga/mutect), Somatic Sniper v1.0.4.2 (gmt.genome.wustl.edu/packages/somatic-sniper), Strelka v1 (sites.google.com/site/strelkasomaticvariantcaller), and Varscan v2.3.8 (varscan.sourceforge.net). SNVs that were identified by at least 2 different callers, with >10% variant allelic fraction and >7x coverage in tumor, and ≥15x coverage with >97% normal allelic fraction in normal, were considered high-confidence variants.

SNVs that did not meet these criteria, but had ≥4x coverage, >6% variant allelic fraction in tumor, ≥4x normal coverage with >97% normal allelic fraction in normal, and passed manual review via Integrative Genomics Viewer (IGV) v2.3 (broadinstitute.org/igv), were considered low-confidence variants. Insertions and deletions (indels) were detected by Strelka and VarScan. Variants that passed manual review in IGV, with ≥4x tumor allelic coverage, >10% tumor allelic fraction, ≥4x normal DNA coverage, and >97% normal allelic fraction were considered as potential indels.

Validation of mutations

All potential indels and low-confidence SNVs, a random selection (15%) of the high-confidence SNVs, and the *TERT* gene promoter were subjected to orthogonal validation using NimbleGen SeqCap EZ target enrichment (Roche), using 500x and 250x sequencing depth for tumor and normal DNA, respectively. Variants with >100x of tumor and normal DNA coverage, >15% variant allelic fraction in tumor, and <3% variant allelic fraction in normal DNA, were considered validated. The overall validation rate in high-confidence SNVs was 96.2%. Validated indels and low confidence SNVs, as well as all high-confidence SNVs, were included in subsequent analyses.

Copy number analysis and tumor purity estimation

Allele-specific copy number data was acquired by analysis of whole exome sequencing bam files using OncoSNP-SEQ (sites.google.com/site/oncosnpseq). Chromosome arm-level alterations and statistically significant amplifications and deletions were determined and visualized using GISTIC 2.0 (broadinstitute.org/cancer/cga/gistic). To determine tumor purity, we analyzed RNA sequencing data using the ESTIMATE algorithm (20).

Gene expression analysis

For SDC samples, raw FASTQ files were aligned to the hg19 genome using STAR aligner with default parameters (21). Aligned fragments were counted with Rsamtools v3.2 and annotated using the TxDb.Hsapiens.UCSC.hg19.knownGene version 3.2 transcript database. The raw count matrix for 591 PAM50-annotated breast cancers published by The Cancer Genome Atlas (TCGA) (22) was downloaded from the TCGA Genome Data Analysis Center (GDAC) firehose (doi:10.7908/C11G0KM9) and merged with the SDC count matrix. Regularized-logarithm transformation of the matrix was obtained with the rlog function of DeSeq2 v1.10.1 after removing the batch effect using the svaseq function of the sva package v3.18.0. FPKM were obtained with DESeq2 using the robust method. The 100 genes with the highest variance of rlog transformed data across both breast and SDC samples were selected and clustered together using a Euclidean distance to define molecular subtypes.

Unsupervised consensus clustering of SDCs and 109 Basal-like breast cancer samples was performed using ConsensusClusterPlus package v1.22.0. The number of clusters was determined empirically according to the consensus index and delta provided in the package. Gene set enrichment analysis of the different clusters was performed using the Farmer et al. breast cancer signatures 1 through 7 (23).

Immunohistochemical analysis

Sections of formalin-fixed, paraffin embedded tumor tissue were stained with androgen receptor antibody clone AR-441 (monoclonal mouse, dilution 1:100; Dako), and were considered positive if immunoreactivity was detected in ≥5% of tumor cell nuclei. ERBB2 staining was done using the anti-HER-2/neu antibody, clone 4B5 (monoclonal rabbit; Roche), and were visualized using the Ultra View Universal DAB detection kit (Ventana Medical Systems). S100 was detected using antibody GA504 (polyclonal rabbit, dilution 1:8000; Dako).

Fluorescence in-situ hybridization (FISH)

Formalin-Fixed Paraffin-Embedded (FFPE) tissue samples were tested for NTRK3 rearrangements by a break-apart FISH assay using a commercial *NTRK3* break-apart FISH probe (Empire Genomics). Four-micron (4 μm) FFPE tissue sections generated from FFPE blocks of tumor specimens were pretreated by deparaffinizing in xylene and dehydrating in ethanol. Dual-color FISH assay was conducted according to the protocol for FFPE sections from Vysis/Abbott Molecular with a few modifications. FISH analysis and signal capture were conducted on a fluorescence microscope (Zeiss) coupled with ISIS FISH Imaging System (Metasystems). We analyzed 100 interphase nuclei from each tumor specimen.

Detection of AR-V7

The AR locus of the RNA sequencing data was displayed with Sashimi plots in IGV 2.3. A sample was reported as androgen receptor splice variant 7 (AR-V7) positive if at least two uniquely aligned junction reads spanning exon 3 and the downstream cryptic exon (expressed intronic region CE3) were detected, with a minimum of 5 nucleotide overhang on either side without mismatches. The number of reads spanning AR-V7 variant splice junctions was normalized to the total number of reads aligned to the reference transcriptome.

PCR analyses

For validation of fusion genes and expression of the AR-V7 splice variant, cDNA was synthesized from tumor RNA using Superscript III Reverse Transcriptase (ThermoFisher Scientific), amplified by PCR and visualized on a 1.5% agarose gel. For validation of fusion genes with intronic breakpoints, PCR was performed using tumor genomic DNA. All primer sequences are listed in Supplementary Table 2.

Androgen receptor signaling analysis

To generate an androgen receptor signaling index, we calculated the average z-score of 46 canonical target genes that are up-regulated by the androgen receptor (Human Androgen Receptor Signaling Targets PCR Array, Qiagen), calculated from FPKM data.

Results and Discussion

Genetic landscape of salivary duct carcinoma

To investigate the spectrum of somatic genetic alterations in SDC, we performed whole-exome sequencing of snap-frozen tumor and matched normal DNA from 16 patients (see

Table 1 for clinical information). The mean coverage was 143x and 74x for tumor and normal DNA respectively, with 98% of the target sequence covered to at least 20x depth (Supplementary Figure 1). We also performed RNA sequencing, with an average of 170M total reads, of which 88% were aligned to the mapping sequence with high quality (Supplementary Figure 2). Orthogonal resequencing showed a high validation rate (>96%) of the mutations detected, and only high confidence and/or validated mutations were included in subsequent analyses (see methods). The average estimated tumor purity was 68% (range: 52–93%), which is higher than reported for most tumor types including breast cancer (20).

We detected a median of 50 non-silent somatic mutations per tumor, corresponding to approximately 1.7 mutations per megabase (Figure 1 and Supplementary Table 3). This places the mutational load of SDC in the lower one-third of solid tumors, close to breast cancer as well as pancreas, prostate, and kidney cancers (24). This mutational burden is higher than that of adenoid cystic carcinoma of the salivary gland, which has 0.3 mutations per megabase (25). In total, 86% were missense mutations, 12% truncating mutations, 2% splice site mutations, and 0.6% in-frame indels. RNA sequencing detected 50% of all mutations, but 94% of mutations in the COSMIC database occurring in cancer genes (Supplementary Figure 3A). The latter group mostly contained mutations with evidence supporting likely importance as drivers of oncogenesis, suggesting that such alterations may be commonly expressed and detected by RNA sequencing. The variant allele frequencies in this group of mutations were higher in RNA than in DNA (Supplementary Figure 3B), which is in line with a previous study (26), and supports the hypothesis that many transforming mutations are highly expressed in tumor cells.

Copy number alterations

We noted a relatively low rate of copy number alterations (CNAs), with amplifications or deletions on chromosome arm-level occurring in 5 patients. The only recurrent arm-level CNA was 8q amplification, present in 3 of 16 (19%) patients (Figure 1), which is in line with previous findings in estrogen receptor-negative breast cancer and head and neck squamous cell carcinoma (22, 27). The 8q arm contains oncogenes such as *MYC*, which has shown recurrent amplifications associated with poor prognosis in several tumor types including prostate cancer (28), and *PLAG1*, which is rearranged and overexpressed in a majority of pleomorphic adenomas (29). Significant focal amplifications included loci 17q12 (including *ERBB2*) and 10q11.21 (including *RET*) in 4 and 1 of 11 patients, respectively (Supplementary Figure 4).

Fusion genes

Unique fusion genes were detected in 5 of 16 patients using RNA sequencing, and were all confirmed by PCR analysis (Figure 1, Supplementary Figure 5). One patient had an *ETV6-NTRK3* fusion, which is found in a majority of mammary analogue secretary carcinoma (MASC) tumors (30). The fusion gene included *ETV6* exons 1–4 and *NTRK3* exons 14–20, which is different from the most common fusion variant (where the breakpoints are located in ETV6 exon 5 and NTRK3 exon 15), but has been previously reported in MASC (31). FISH analysis showed rearrangement of the *NTRK3* locus in 92% of the cells

(Supplementary Figure 6D). To confirm the SDC diagnosis, we re-reviewed additional tissue sections and noted typical SDC morphology (Supplementary Figure 6A–C), which is distinct from that of MASC (32). Furthermore, the tumor was positive for AR and negative for S100, which have been previously detected in 0/9 and 15/15 cases of MASC, respectively (33). Although the *ETV6-NTRK3* fusion has been reported in breast secretory carcinoma and sporadically in other diseases such as congenital mesoblastic nephroma, congenital fibrosarcoma, and acute myeloid leukemia (30), it has not been detected in salivary gland tumors other than MASC. This finding may suggest that the *ETV6-NTRK3* fusion is not pathognomonic for MASC. An alternative explanation could be that this case was initially a MASC that underwent a transformation with the emergence of a high-grade SDC-like tumor. However, this appears unlikely considering the absence of MASC histology or IHC findings in the tumor, and that no previously reported cases of MASC with high grade transformation have shown SDC morphology. This case also demonstrates the potential clinical value of tumor sequencing, because the *ETV6-NTRK3* fusion is targetable. Our group recently reported a near-complete response to TRK inhibition in a patient whose salivary carcinoma harbored a similar *ETV6-NTRK3* fusion gene (34).

Two patients with SDC ex-PA had *CTNNB1-PLAG1* or *LIFR-PLAG1* fusions, which have been previously described in pleomorphic adenoma (30). Another patient had a *BCL6-TRADD* fusion gene. *BCL6* is commonly translocated in diffuse large B cell lymphoma (35), but has never been reported with *TRADD* as fusion partner. Finally, one tumor harbored an *ABL1-PPP2R2C* fusion. Rearrangements including the 3′ portion of *ABL1* with several different 5′ fusion partners are found in hematological malignancies (36). However, the reciprocal *PPP2R2C-ABL1* fusion was not detected by RT-PCR.

Recurrent genetic alterations

Recurrent mutations and CNAs are depicted in Figure 1A. We interrogated selected genes in a second cohort, consisting of 15 patients with recurrent or metastatic SDC, whose tumors were analyzed using MSK-IMPACT, a clinical sequencing assay designed to detect potentially targetable mutations and copy number alterations in 410 cancer-related genes (Supplementary Figure 7A and Supplementary Table 4 for results, and Supplementary Table 5 for clinical information) (16). Overall, SDC showed a relatively low number of mutations and CNAs compared to other tumor types that were analyzed using the same platform (Supplementary Figure 7B), which is in line with our findings in cohort 1.

Across both cohorts (n=31), *TP53* alterations were most prevalent and were detected in 17 (55%) cases (Figure 1B). The frequency of *TP53* alterations was higher in cohort 2 than in cohort 1 (80% vs 31%, OR=8.8, P=0.011; Fisher's exact test), suggesting that this mutation may be enriched in tumors that behave aggressively, since all cohort 2 tumors were recurrent/metastatic.

Amplification of *ERBB2* was detected in 10 of 31 (32%) cases, which is similar to previous SDC studies (3, 5, 10, 11). The ERBB2 inhibitor trastuzumab is used as standard treatment of *ERBB2* amplified breast cancer (37), and has been tested with promising results in SDC (12–14). In our study, 3 patients with *ERBB2* amplification were treated with trastuzumab in combination with chemotherapy. One patient received trastuzumab for 1 year as part of

adjuvant therapy and had no sign of disease at follow-up 6 years later, one was alive with stable bone metastases after receiving trastuzumab as maintenance treatment for 4 years, and one was enrolled on a clinical trial with an anti-PD1 antibody after experiencing progression of disease after 1 year of trastuzumab treatment. Alterations leading to activation of the PI3K/AKT/mTOR pathway may cause ERBB2 inhibitor resistance in breast cancer (38), and *AKT1* amplifications, *RPTOR* amplification/mutations or truncating *PTEN* mutations were detected in 4 of 10 *ERBB2* amplified tumors (Figure 1 and Supplementary Figure 7A). Our findings warrant further studies to investigate the effect of such alterations on response to ERBB2 inhibition in SDCs harboring *ERBB2* gene amplification.

Of note, most tumors (74%) had mutations in either the mitogen-activated protein kinase (MAPK) pathway (*BRAF*, *HRAS* and *NF1*), or in *ERBB2* (*P* for mutual exclusivity = 0.057, Fisher's exact test). This indicates that *ERBB2* amplification and MAPK pathway activation are the predominating drivers of oncogenesis in SDC, and may act through independent or redundant mechanisms.

Seven of 31 (23%) patients harbored activating *HRAS* mutations. Interestingly, 3 of 3 patients with an *HRAS* G13R mutation also had a co-occurring PIK3CA H1047R mutation. On the other hand, no *PIK3CA* mutation was detected in the 4 patients with HRAS Q61R (p=.029; Supplementary Table 6). These data suggest that HRAS Q61R might be a more potently activating mutation, whereas HRAS G13R cooperates with PIK3CA H1047R to promote oncogenesis in SDC. Similar findings have been observed in other cancer types, where *PIK3CA* has been shown to cooperate with specific *RAS* mutations (39), in a manner that can generate dependency on PI3K signalling and resistance to ERBB2 inhibition. These data may have relevance for the targeting of *PIK3CA* or *ERBB2* in SDC.

Mutations in the promoter region of the human telomerase reverse transcriptase (*TERT*) gene occur in several cancer types (40). We sequenced the *TERT* promoter and found no mutations in any of 31 tumors, suggesting that these alterations are rare in SDC.

In total, 21 of 31 (70%) patients had a history of tobacco smoking. There were no associations between smoking status and any genetic alterations detected in the study. There were also no significant associations between the above-described genetic alterations and overall or recurrence-free survival (data not shown).

Actionability of alterations

To investigate the clinical relevance of molecular characterization in SDC patients, we categorized alterations according to levels of evidence supporting standard or investigative therapies. There were no alterations that have standard of care therapeutic implications, since there are no FDA-approved drugs or biomarkers in SDC. However, 19 tumors (61%) had alterations that were potentially actionable, because the specific alteration corresponded to either an FDA-approved treatment, or to a treatment with published clinical evidence in another cancer type. An additional 3 tumors (10%) contained alterations in which preclinical studies suggest potential activity of such drugs (Figure 1C and Supplementary Table 7).

Taken together, a high percentage of SDCs have actionable alterations with supportive clinical evidence. These findings are in stark contrast to the two other salivary cancer types that have been genetically profiled – adenoid cystic carcinomas and polymorphous low-grade adenocarcinomas – which both have a relative paucity of actionable targets (25, 41). Therefore, routine clinical tumor sequencing in SDCs may yield potentially actionable information.

Alterations affecting androgen receptor signaling

Immunohistochemistry showed positive staining for AR in 12 of 16 (75%) cases (Figure 1). Since androgen deprivation therapy (ADT) has been suggested as potential treatment for AR-positive SDC (8, 9), we investigated potential molecular mechanisms of ADT resistance in these tumors. The androgen receptor splice variant 7 (AR-V7), including AR exons 1–3 and a cryptic exon 3 (CE3) instead of 1–8 (Figure 2A), has been detected in prostate cancer and is associated with ADT resistance (42). AR-V7 lacks the ligand binding domain but is transcriptionally active. Analysis of the RNA sequencing data showed evidence of AR-V7 expression in 8 of 16 cases. When compared to full length AR, the ratios of AR-V7 (mean 5.1%, range 0.5–15.1% of total AR reads) were comparable to those detected in prostate cancer (Figure 2B–C) (43). Expression of AR-V7 was confirmed by RT-PCR in 7 of the 8 cases (Figure 2C). This confirms data from a prior study identifying AR-V7 in SDC (44), and additionally demonstrate that in many cases, the ratios of AR-V7 are quite low in comparison to full-length AR. These results suggest that future clinical trials investigating ADT in SDC should incorporate assessment of the presence, and ratios of AR-V7, in tumors before and during/after treatment, and that RNA sequencing is a more sensitive measure than RT-PCR.

Forkhead box protein A1 (*FOXA1*) is a pioneer transcription factor that acts by binding to and exposing chromatin, thereby enabling AR and other hormone receptors to activate transcription of their target genes. In prostate cancer, AR and FOXA1 protein levels correlate with each other, and high FOXA1 levels are associated with poor prognosis and the development of metastasis (45). In SDC, we also noted a strong correlation between *FOXA1* and *AR* mRNA levels in SDC tumors (Figure 2D).

Although functional studies are lacking, clinical data have suggested that *FOXA1* mutations may be associated with ADT resistance (46). Three SDC patients had *FOXA1* mutations, which did not appear to affect AR expression levels (Figure 2D). Like most *FOXA1* mutations found in ADT-resistant prostate cancer (46), these were all located in the DNA binding domain (Figure 2E). To investigate the effect of the *FOXA1* mutations on AR activity, we compared *AR* mRNA levels to a composite estimate of AR signaling, derived from the average expression of 46 canonical genes upregulated by AR (*see Methods*). AR signaling correlated with AR expression at both protein and mRNA levels. Interestingly, the tumor with a Q263-C268 FOXA1 deletion showed low AR signaling despite the highest AR expression of all cases (Figure 2F and G). This suggests that the Q263-C268 deletion represses AR signaling, although these data are preliminary and the hypothesis requires additional confirmation. Nevertheless, the presence of *FOXA1* mutations in SDC is likely to have significant implications as ADT is investigated in SDC.

We also detected two missense mutations, one frameshift insertion and one amplification of the fatty acid synthase (*FASN*) gene. Overexpression of *FASN* is prevalent in several tumor types and been proposed as a potential ADT resistance mechanism in prostate cancer (47), although mechanistic data remain lacking.

In our study, 4 patients with AR-positive tumors and recurrent disease received ADT treatment with or without chemotherapy. Of these patients, 3 developed progression of disease and 1 currently remains on therapy with stable disease after 17 months.

SDC resembles molecular apocrine breast cancer

Morphologically, SDC resembles invasive ductal carcinoma of the breast, and the two diseases share some immunohistochemical features such as AR and ERBB2 expression, which are seen in 58–87% and 20% of breast cancers, respectively (6, 7, 48). Thus it is possible that SDC and breast cancer may be molecularly similar. However, this has not been previously investigated at the scale of global gene expression.

We performed unsupervised hierarchial clustering based on gene expression data from RNA sequencing in the 16 cases of SDC and 591 breast cancers sequenced by TCGA (22). Despite arising from a different organ, the SDC tumors did not cluster separately from the breast cancers. Instead, they clustered together with basal-like and HER2-enriched breast tumors, and separately from Luminal A, Luminal B and normal-like breast tumors (Figure 3A). As has been suggested based on IHC data (4, 6), we found that SDCs could be divided into three groups based on *AR* and *ERBB2* gene expression. Four tumors had low *AR* and *ERBB2* levels, 8 tumors had high *AR* and low *ERBB2*, and 4 tumors had high *AR* and *ERBB2* (Figure 3B). Interestingly, 3 of 4 SDCs with low *AR* and *ERBB2* expression clustered with basal-like breast cancers, whereas *AR*-high cases, regardless of *ERBB2* status, predominately clustered with *ERBB2*-enriched breast cancers (Figure 3C). These findings indicate that SDC shows a distinct similarity to breast cancer not only by histology and immunohistochemistry, but also by global gene expression patterns.

To determine which breast cancer subtype SDC is closest to based on molecular profile, we then performed consensus clustering of the SDCs and 109 basal-like breast tumors from TCGA according to methods described by Lehmann et al. (49). Similar to that study, we detected an optimal number of 7 clusters (Supplementary Figure 8). All SDC cases were classified together with a subset of the breast tumors forming cluster 1 (Figure 4A). To explore the nature of this cluster, we performed gene set enrichment analysis (GSEA), using gene sets specific for different subtypes of breast cancer as defined by Farmer et al. (23). The differentially expressed genes associated with tumors of cluster 1 showed a significant enrichment for Farmer's gene cluster 7 ($P<0.0001$), which defines the molecular apocrine subtype of breast cancer (Figure 4B). There was no significant overlap with any other of Farmer's gene clusters (Figure 4C).

Of note, all SDCs were classified in the cluster of molecular apocrine-like tumors, regardless of AR status. This raises the possibility that AR-negative tumors have alternative mechanisms for the activation of AR target genes. Indeed, 3 of 4 tumors negative for AR gene expression had a high to average AR signaling index (Figure 2G). GSEA analysis of

genes differentially expressed in the 12 AR-positive compared to 4 AR-negative SDCs revealed a strong enrichment of genes dysregulated by androgen stimulation of the molecular apocrine breast cancer cell line MDA-MB-453 (Supplementary Figure 9) (50), further indicating that the two cancer types respond to androgens in a similar fashion. A clinical trial evaluating ADT in AR-positive breast cancer is ongoing (NCT01889238), and may give further insights to molecular markers of response to this treatment.

Conclusions

To our knowledge, this is the first study to comprehensively analyze genetic alterations and gene expression features in SDC, providing a rationale for future targeted therapy trials. Our results illuminate the unique biology of SDC, identify a high prevalence of actionable molecular alterations, and have direct implications for clinical trials.

SDCs are aggressive salivary cancers, with no highly active systemic therapy, and no predictive biomarkers. The majority of tumors are ultimately treatment-resistant and lethal. Our results show that the majority (61%) of SDCs have alterations with published clinical evidence supporting specific targeted therapies. In the emerging era of precision oncology and biomarker-defined basket studies, these data suggest that routine clinical tumor sequencing for this disease is likely to be of high clinical value.

Our results suggest that ADT could be investigated in the majority of SDCs, and ERBB2 inhibition in a subset of the patients. We found evidence supporting several potential mechanisms of resistance to these drugs, such as AR-V7 expression and *FOXA1* mutations in AR-positive tumors, and PI3K-AKT pathway alterations in cases with *ERBB2* amplification. It will be important to assess these genetic and expression-based biomarkers in correlative analyses for patients enrolled on ADT or ERBB2 inhibitor trials.

These data also define the diverse molecular landscape of SDC. For example, we describe the first occurrence of the *ETV6-NTRK3* fusion gene in a tumor with histologic features and IHC profile typical of SDC.

Finally, we show that the gene expression pattern of SDC is highly similar to that of molecular apocrine breast carcinoma. This has long been speculated based on similarities in IHC, but has not heretofore been confirmed at the level of genome-wide data. It is likely that parallel clinical investigation of ADT and other treatments in apocrine breast cancer will generate useful data and hypotheses for SDC trials, which are currently constrained by the rarity of this cancer.

Supplementary Material

Refer to Web version on PubMed Central for supplementary material.

Acknowledgments

We thank R. Ghossein for expert head and neck pathology tumor review; T. Nielsen for graphic design; G. Stenman, M. Persson, PA. Watson, E. Adams and H. Hieronymus for discussions and technical assistance.

Financial support: This work was supported by NIH P30 CA008748. M.G.D was supported by Sahlgrenska University Hospital, The Gothenburg Medical Society, The Swedish Society of Medicine, and Svensson's Fund for Medical Research. L.G.T.M. was supported by the Damon Runyon Cancer Research Foundation, NIH K08 DE024774, and the Society of MSK. T.A.C. was supported by grants from the Adenoid Cystic Carcinoma Research Foundation and the Geoffrey Beene Cancer Center.

References

1. Jayaprakash V, Merzianu M, Warren GW, Arshad H, Hicks WL Jr, Rigual NR, et al. Survival rates and prognostic factors for infiltrating salivary duct carcinoma: Analysis of 228 cases from the Surveillance, Epidemiology, and End Results database. Head Neck. 2014; 36(5):694–701. [PubMed: 23606370]
2. Otsuka K, Imanishi Y, Tada Y, Kawakita D, Kano S, Tsukahara K, et al. Clinical Outcomes and Prognostic Factors for Salivary Duct Carcinoma: A Multi-Institutional Analysis of 141 Patients. Ann Surg Oncol. 2016
3. Luk PP, Weston JD, Yu B, Selinger CI, Ekmejian R, Eviston TJ, et al. Salivary duct carcinoma: Clinicopathologic features, morphologic spectrum, and somatic mutations. Head Neck. 2015
4. Simpson RH. Salivary duct carcinoma: new developments--morphological variants including pure in situ high grade lesions; proposed molecular classification. Head Neck Pathol. 2013; 7(Suppl 1):S48–58. [PubMed: 23821208]
5. Chiosea SI, Williams L, Griffith CC, Thompson LD, Weinreb I, Bauman JE, et al. Molecular characterization of apocrine salivary duct carcinoma. Am J Surg Pathol. 2015; 39(6):744–52. [PubMed: 25723113]
6. Di Palma S, Simpson RH, Marchio C, Skalova A, Ungari M, Sandison A, et al. Salivary duct carcinomas can be classified into luminal androgen receptor-positive, HER2 and basal-like phenotypes. Histopathology. 2012; 61(4):629–43. [PubMed: 22882517]
7. Grogg A, Trippel M, Pfaltz K, Ladrach C, Droeser RA, Cihoric N, et al. Androgen receptor status is highly conserved during tumor progression of breast cancer. BMC cancer. 2015; 15:872. [PubMed: 26552477]
8. Locati LD, Quattrone P, Bossi P, Marchiano AV, Cantu G, Licitra L. A complete remission with androgen-deprivation therapy in a recurrent androgen receptor-expressing adenocarcinoma of the parotid gland. Ann Oncol. 2003; 14(8):1327–8. [PubMed: 12881399]
9. Jaspers HC, Verbist BM, Schoffelen R, Mattijssen V, Slootweg PJ, van der Graaf WT, et al. Androgen receptor-positive salivary duct carcinoma: a disease entity with promising new treatment options. J Clin Oncol. 2011; 29(16):e473–6. [PubMed: 21422415]
10. Johnson CJ, Barry MB, Vasef MA, Deyoung BR. Her-2/neu expression in salivary duct carcinoma: an immunohistochemical and chromogenic in situ hybridization study. Appl Immunohistochem Mol Morphol. 2008; 16(1):54–8. [PubMed: 18091319]
11. Skalova A, Starek I, Vanecek T, Kucerova V, Plank L, Szepe P, et al. Expression of HER-2/neu gene and protein in salivary duct carcinomas of parotid gland as revealed by fluorescence in-situ hybridization and immunohistochemistry. Histopathology. 2003; 42(4):348–56. [PubMed: 12653946]
12. Limaye SA, Posner MR, Krane JF, Fonfria M, Lorch JH, Dillon DA, et al. Trastuzumab for the treatment of salivary duct carcinoma. Oncologist. 2013; 18(3):294–300. [PubMed: 23429737]
13. Lee JS, Kwon OJ, Park JJ, Seo JH. Salivary duct carcinoma of the parotid gland: is adjuvant HER-2-targeted therapy required? J Oral Maxillofac Surg. 2014; 72(5):1023–31. [PubMed: 24480767]
14. Kadowaki S, Yatabe Y, Hirakawa H, Komori A, Kondoh C, Hasegawa Y, et al. Complete Response to Trastuzumab-Based Chemotherapy in a Patient with Human Epidermal Growth Factor Receptor-2-Positive Metastatic Salivary Duct Carcinoma ex Pleomorphic Adenoma. Case Rep Oncol. 2013; 6(3):450–5. [PubMed: 24163659]
15. Ku BM, Jung HA, Sun JM, Ko YH, Jeong HS, Son YI, et al. High-throughput profiling identifies clinically actionable mutations in salivary duct carcinoma. J Transl Med. 2014; 12:299. [PubMed: 25343854]

16. Hyman DM, Solit DB, Arcila ME, Cheng DT, Sabbatini P, Baselga J, et al. Precision medicine at Memorial Sloan Kettering Cancer Center: clinical next-generation sequencing enabling next-generation targeted therapy trials. Drug Discov Today. 2015; 20(12):1422–8. [PubMed: 26320725]
17. Jun G, Flickinger M, Hetrick KN, Romm JM, Doheny KF, Abecasis GR, et al. Detecting and estimating contamination of human DNA samples in sequencing and array-based genotype data. Am J Hum Genet. 2012; 91(5):839–48. [PubMed: 23103226]
18. Li H, Durbin R. Fast and accurate short read alignment with Burrows-Wheeler transform. Bioinformatics. 2009; 25(14):1754–60. [PubMed: 19451168]
19. DePristo MA, Banks E, Poplin R, Garimella KV, Maguire JR, Hartl C, et al. A framework for variation discovery and genotyping using next-generation DNA sequencing data. Nat Genet. 2011; 43(5):491–8. [PubMed: 21478889]
20. Yoshihara K, Shahmoradgoli M, Martinez E, Vegesna R, Kim H, Torres-Garcia W, et al. Inferring tumour purity and stromal and immune cell admixture from expression data. Nat Commun. 2013; 4:2612. [PubMed: 24113773]
21. Dobin A, Davis CA, Schlesinger F, Drenkow J, Zaleski C, Jha S, et al. STAR: ultrafast universal RNA-seq aligner. Bioinformatics. 2013; 29(1):15–21. [PubMed: 23104886]
22. Comprehensive molecular portraits of human breast tumours. Nature. 2012; 490(7418):61–70. [PubMed: 23000897]
23. Farmer P, Bonnefoi H, Becette V, Tubiana-Hulin M, Fumoleau P, Larsimont D, et al. Identification of molecular apocrine breast tumours by microarray analysis. Oncogene. 2005; 24(29):4660–71. [PubMed: 15897907]
24. Lawrence MS, Stojanov P, Polak P, Kryukov GV, Cibulskis K, Sivachenko A, et al. Mutational heterogeneity in cancer and the search for new cancer-associated genes. Nature. 2013; 499(7457): 214–8. [PubMed: 23770567]
25. Ho AS, Kannan K, Roy DM, Morris LG, Ganly I, Katabi N, et al. The mutational landscape of adenoid cystic carcinoma. Nat Genet. 2013; 45(7):791–8. [PubMed: 23685749]
26. Wilkerson MD, Cabanski CR, Sun W, Hoadley KA, Walter V, Mose LE, et al. Integrated RNA and DNA sequencing improves mutation detection in low purity tumors. Nucleic Acids Res. 2014; 42(13):e107. [PubMed: 24970867]
27. Comprehensive genomic characterization of head and neck squamous cell carcinomas. Nature. 2015; 517(7536):576–82. [PubMed: 25631445]
28. Fromont G, Godet J, Peyret A, Irani J, Celhay O, Rozet F, et al. 8q24 amplification is associated with Myc expression and prostate cancer progression and is an independent predictor of recurrence after radical prostatectomy. Hum Pathol. 2013; 44(8):1617–23. [PubMed: 23574779]
29. Katabi N, Ghossein R, Ho A, Dogan S, Zhang L, Sung YS, et al. Consistent PLAG1 and HMGA2 abnormalities distinguish carcinoma ex-pleomorphic adenoma from its de novo counterparts. Hum Pathol. 2015; 46(1):26–33. [PubMed: 25439740]
30. Stenman G. Fusion oncogenes in salivary gland tumors: molecular and clinical consequences. Head Neck Pathol. 2013; 7(Suppl 1):S12–9. [PubMed: 23821214]
31. Skalova A, Vanecek T, Simpson RH, Laco J, Majewska H, Baneckova M, et al. Mammary Analogue Secretory Carcinoma of Salivary Glands: Molecular Analysis of 25 ETV6 Gene Rearranged Tumors With Lack of Detection of Classical ETV6-NTRK3 Fusion Transcript by Standard RT-PCR: Report of 4 Cases Harboring ETV6-X Gene Fusion. Am J Surg Pathol. 2016; 40(1):3–13. [PubMed: 26492182]
32. Stevens TM, Kovalovsky AO, Velosa C, Shi Q, Dai Q, Owen RP, et al. Mammary analog secretory carcinoma, low-grade salivary duct carcinoma, and mimickers: a comparative study. Mod Pathol. 2015; 28(8):1084–100. [PubMed: 26089091]
33. Skalova A, Vanecek T, Sima R, Laco J, Weinreb I, Perez-Ordonez B, et al. Mammary analogue secretory carcinoma of salivary glands, containing the ETV6-NTRK3 fusion gene: a hitherto undescribed salivary gland tumor entity. Am J Surg Pathol. 2010; 34(5):599–608. [PubMed: 20410810]
34. Drilon A, Li G, Dogan S, Gounder M, Shen R, Arcila M, et al. What hides behind the MASC: Clinical response and acquired resistance to entrectinib after ETV6-NTRK3 identification in a mammary analogue secretory carcinoma (MASC). Ann Oncol. 2016

35. Iqbal J, Greiner TC, Patel K, Dave BJ, Smith L, Ji J, et al. Distinctive patterns of BCL6 molecular alterations and their functional consequences in different subgroups of diffuse large B-cell lymphoma. Leukemia. 2007; 21(11):2332–43. [PubMed: 17625604]
36. De Braekeleer E, Douet-Guilbert N, Rowe D, Bown N, Morel F, Berthou C, et al. ABL1 fusion genes in hematological malignancies: a review. Eur J Haematol. 2011; 86(5):361–71. [PubMed: 21435002]
37. Piccart-Gebhart MJ, Procter M, Leyland-Jones B, Goldhirsch A, Untch M, Smith I, et al. Trastuzumab after adjuvant chemotherapy in HER2-positive breast cancer. New Engl J Med. 2005; 353(16):1659–72. [PubMed: 16236737]
38. Gagliato DM, Jardim DL, Marchesi MS, Hortobagyi GN. Mechanisms of resistance and sensitivity to anti-HER2 therapies in HER2+ breast cancer. Oncotarget. 2016
39. Oda K, Okada J, Timmerman L, Rodriguez-Viciana P, Stokoe D, Shoji K, et al. PIK3CA cooperates with other phosphatidylinositol 3′-kinase pathway mutations to effect oncogenic transformation. Cancer Res. 2008; 68(19):8127–36. [PubMed: 18829572]
40. Heidenreich B, Rachakonda PS, Hemminki K, Kumar R. TERT promoter mutations in cancer development. Curr Opin Genet Dev. 2014; 24:30–7. [PubMed: 24657534]
41. Weinreb I, Piscuoglio S. Hotspot activating PRKD1 somatic mutations in polymorphous low-grade adenocarcinomas of the salivary glands. Nat Genet. 2014; 46(11):1166–9. [PubMed: 25240283]
42. Antonarakis ES, Lu C, Wang H, Luber B, Nakazawa M, Roeser JC, et al. AR-V7 and resistance to enzalutamide and abiraterone in prostate cancer. New Engl J Med. 2014; 371(11):1028–38. [PubMed: 25184630]
43. Robinson D, Van Allen EM, Wu YM, Schultz N, Lonigro RJ, Mosquera JM, et al. Integrative clinical genomics of advanced prostate cancer. Cell. 2015; 161(5):1215–28. [PubMed: 26000489]
44. Mitani Y, Rao PH, Maity SN, Lee YC, Ferrarotto R, Post JC, et al. Alterations associated with androgen receptor gene activation in salivary duct carcinoma of both sexes: potential therapeutic ramifications. Clin Cancer Res. 2014; 20(24):6570–81. [PubMed: 25316813]
45. Sahu B, Laakso M, Ovaska K, Mirtti T, Lundin J, Rannikko A, et al. Dual role of FoxA1 in androgen receptor binding to chromatin, androgen signalling and prostate cancer. EMBO J. 2011; 30(19):3962–76. [PubMed: 21915096]
46. Robinson JL, Holmes KA, Carroll JS. FOXA1 mutations in hormone-dependent cancers. Front Oncol. 2013; 3:20. [PubMed: 23420418]
47. Wen S, Niu Y, Lee SO, Yeh S, Shang Z, Gao H, et al. Targeting fatty acid synthase with ASC-J9 suppresses proliferation and invasion of prostate cancer cells. Mol Carcinogen. 2016
48. Gajria D, Chandarlapaty S. HER2-amplified breast cancer: mechanisms of trastuzumab resistance and novel targeted therapies. Expert Rev Anticancer Ther. 2011; 11(2):263–75. [PubMed: 21342044]
49. Lehmann BD, Bauer JA, Chen X, Sanders ME, Chakravarthy AB, Shyr Y, et al. Identification of human triple-negative breast cancer subtypes and preclinical models for selection of targeted therapies. J Clin Invest. 2011; 121(7):2750–67. [PubMed: 21633166]
50. Doane AS, Danso M, Lal P, Donaton M, Zhang L, Hudis C, et al. An estrogen receptor-negative breast cancer subset characterized by a hormonally regulated transcriptional program and response to androgen. Oncogene. 2006; 25(28):3994–4008. [PubMed: 16491124]

Translational relevance

Salivary duct carcinomas (SDCs) often present with locoregionally advanced disease or distant metastases. The majority of patients ultimately succumb to treatment-resistant disease. Therapies such as androgen-deprivation therapy (ADT) and HER2 inhibition have achieved anecdotal responses, but the rarity of this disease and limited molecular data have impeded the design of rational clinical studies. To date, molecular profiling of SDCs has been restricted to ad hoc analyses of only specific genes. Here, through whole-exome, targeted capture and transcriptome sequencing, we identified many targetable alterations, as well as potential ADT resistance mechanisms. Our analysis also reveals a strong molecular similarity to apocrine breast carcinoma, a tumor type in which ADT has demonstrated activity. Taken together, these data expand our knowledge of the biology of SDC, particularly molecular features that have relevance to ADT, HER2 inhibition, and other targeted therapies.

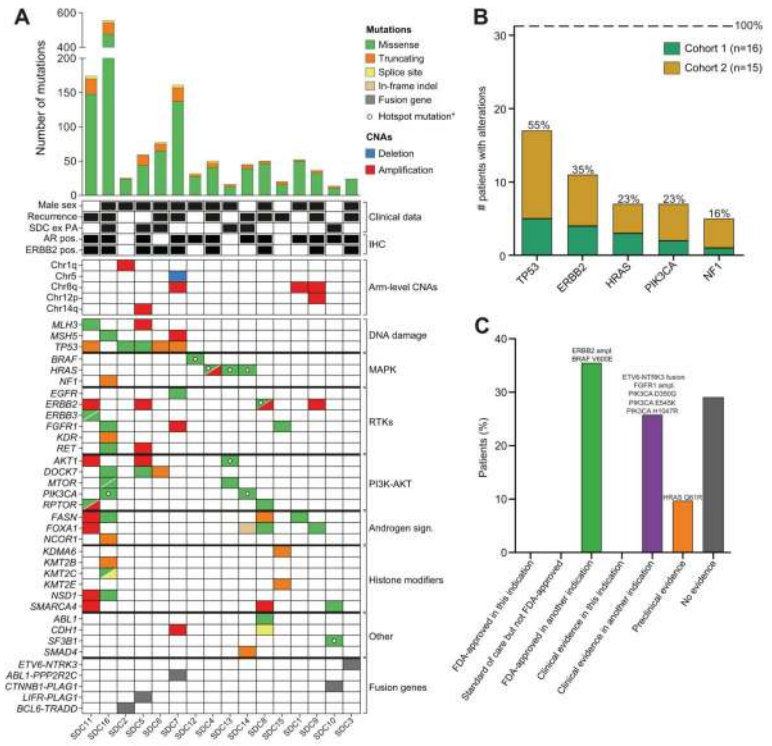

Figure 1.

Genetic landscape of salivary duct carcinoma. (A) Number of somatic mutations (top), clinical data (middle) and selected genetic alterations (bottom) in 16 patients with SDC. SDC ex. PA, Salivary duct carcinoma ex pleomorphic adenoma; AR, Androgen receptor; IHC, Immunohistochemistry; CNA, copy number alteration; MAPK, mitogen-activated protein kinase pathway; RTKs, receptor tyrosine kinases. *Hotspot mutation: At least 20 cases of the mutation reported in the COSMIC database (cancer.sanger.ac.uk/cosmic). (B) Most commonly altered genes in cohorts 1 and 2 combined. Mutations and significant copy number alterations are included. (C) Percent of patients with potentially targetable alterations according to the Memorial Sloan Kettering Cancer Center (MSKCC) levels of evidence, and the specific alterations listed for each category.

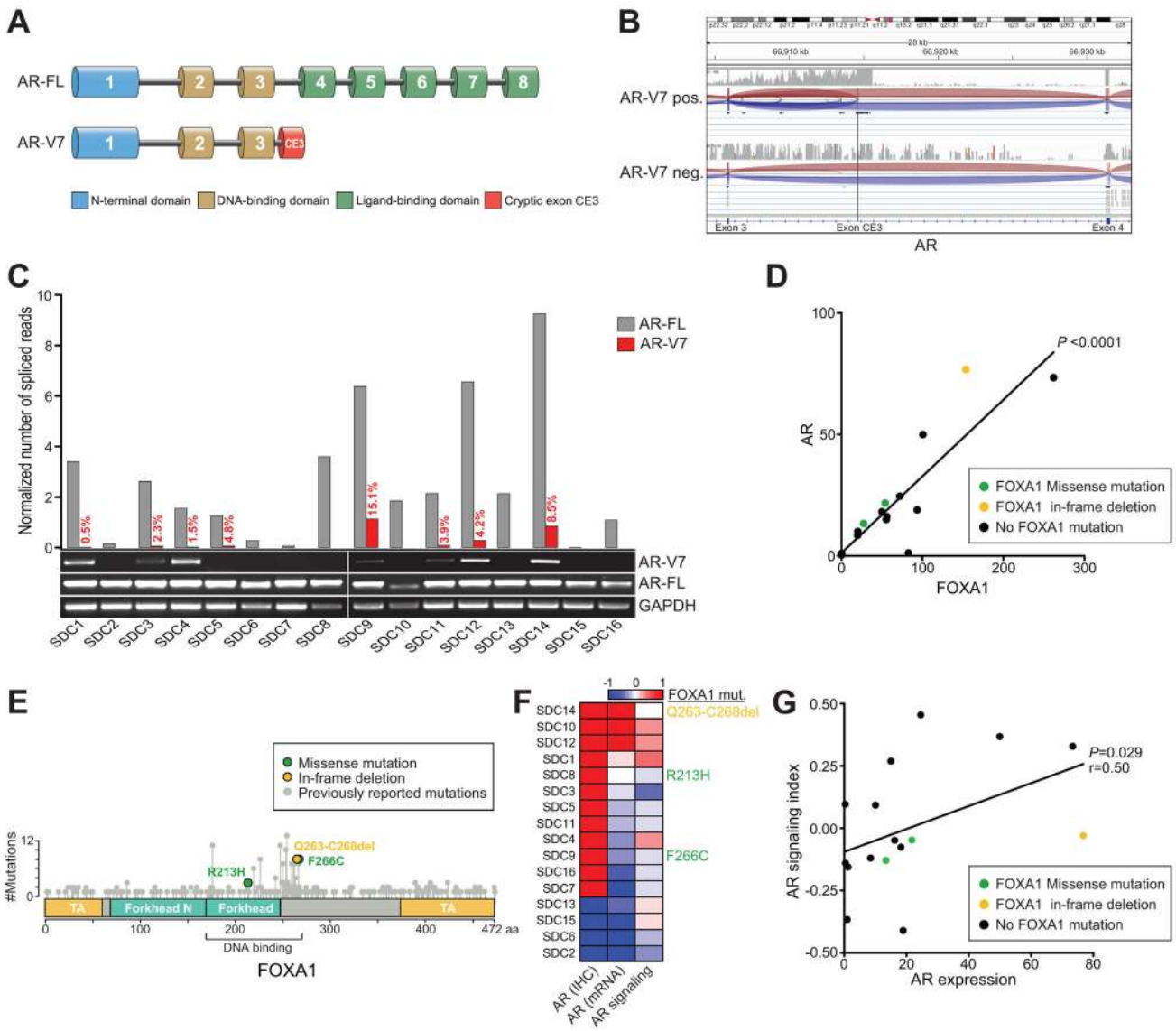

Figure 2.

Alterations related to androgen signaling. (A) Illustration of the androgen receptor (AR) full length (FL) gene, including exons 1–8, and AR transcript variant 7 (V7), including exons 1–3 and cryptic exon 3 (CE3). (B) Sashimi plots showing RNA sequencing reads that span more than one AR exon. Representative cases with (top) or without (bottom) reads spanning exon 3 and CE3 are shown. (C) Quantification of AR-FL and AR-V7 expression based on RNA sequencing (top), and reverse transcriptase-PCR using cDNA extracted from tumor RNA (bottom). (D) Correlation between AR and FOXA1 expression. P<0.0001, 2-tailed Pearson correlation test. (E) Location of SDC mutations within the FOXA1 gene. Previously reported mutations were acquired from the cBioPortal database (cbioportal.org), and represents cases from any cancer. TA, transactivation domain; Forkhead N, Forkhead N-terminal domain. (F) Correlation between AR immunohistochemistry (red, positive; blue, negative), AR expression (based on z-score) and AR signaling index (see methods) with

FOXA1 mutation status. (G) Correlation between AR expression and AR signaling index. *P*, one-tailed Spearman correlation.

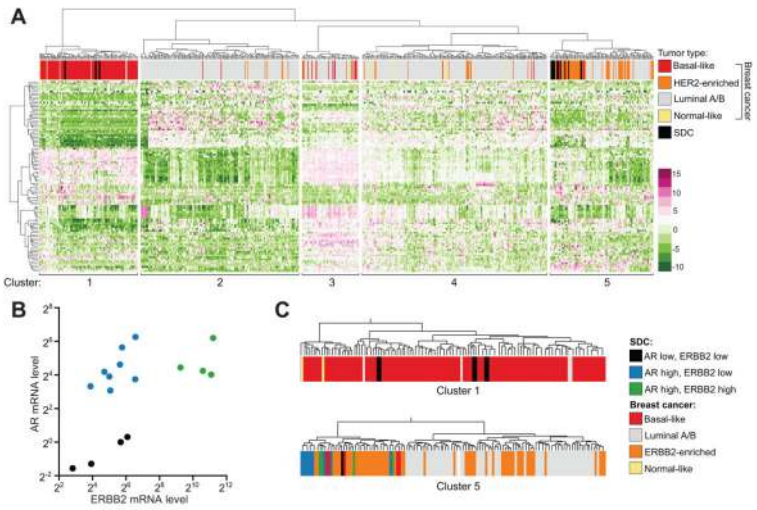

Figure 3.

SDC shows a similar gene expression pattern as estrogen-receptor negative breast cancer. (A) Unsupervised clustering of 16 cases of SDC (blue) and 591 cases of breast cancer from TCGA (x-axis), based on expression of the 100 most variable genes (y-axis). Breast cancer subtype was determined using the PAM50 gene signature. (B) *AR* and *ERBB2* gene expression (FPKM) in SDC tumors based on RNA sequencing. (C) Enlargement of cluster 1 and 5 from figure 3A, with SDC cases colored according to *AR* and *ERBB2* expression.

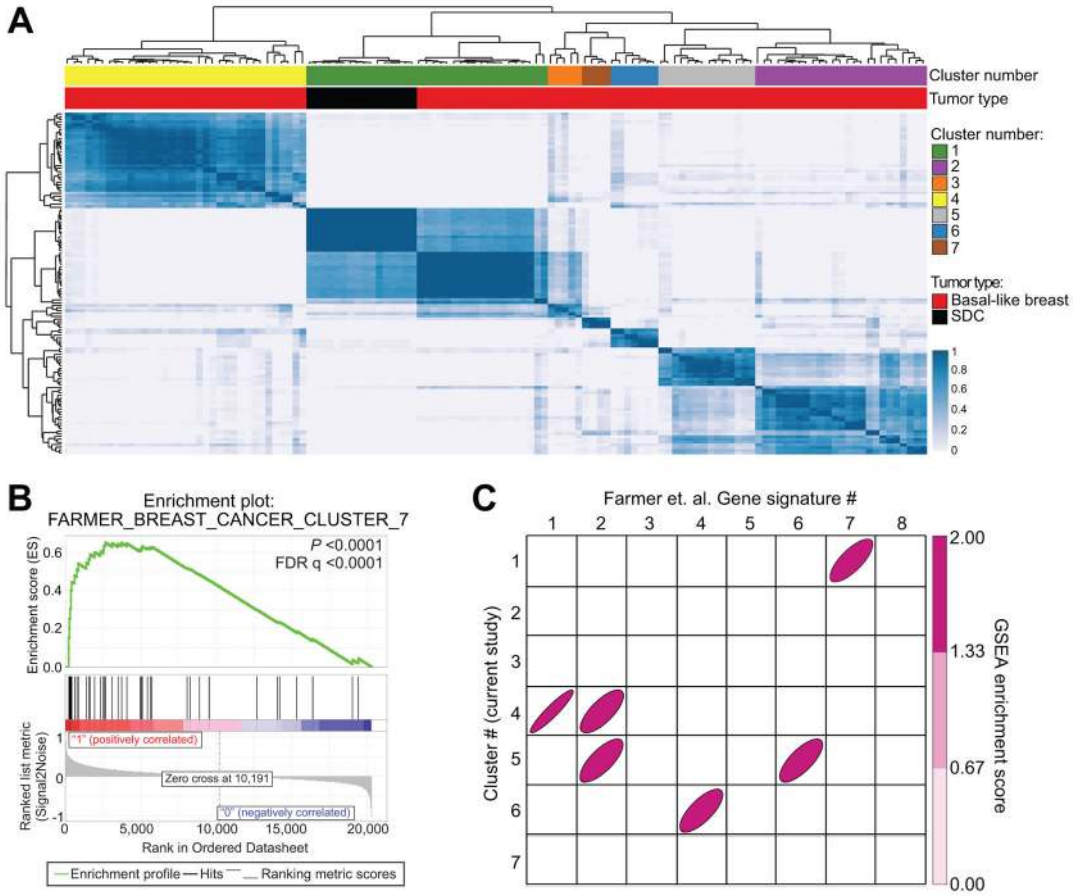

Figure 4.

SDC resembles molecular apocrine breast cancer. (A) Consensus clustering of 16 SDC tumors (blue) and 109 basal-like breast cancers from TCGA (red), defined using the PAM50 gene signature. (B) Gene set enrichment analysis showing an overlap between differentially expressed genes in cluster 1 (from Figure 4A), and gene signature 7 as determined by Farmer et al. FDR, false discovery rate. (C) Gene set enrichment analysis between clusters (from Figure 4A) and gene signatures according to Farmer et al. Ellipses represent significant enrichment of gene sets between two clusters. Ellipse area corresponds to level of significance.

Table 1

Clinical information.

Clinical Feature	n (%) or mean (range)
Male sex	12 (75%)
Age at diagnosis (y)	63 (47–76)
Smoking history	10 (63%)
Primary tumor site	
Parotid	15 (94%)
Submandibular	1 (6%)
Minor glands	0 (0%)
T classification *	
T1–T2	2 (13%)
T3	6 (38%)
T4	8 (50%)
N classification *	
N0	4 (25%)
N1	5 (31%)
N2	7 (44%)
M classification *	
M0	4 (25%)
M1	1 (6%)
MX	11 (69%)
Overall stage *	
III	5 (31%)
IVa	7 (44%)
IVb	3 (19%)
IVc	1 (6%)
Initial therapy	
Surgery+RT	10 (63%)
Surgery+RT+CT	3 (19%)
Surgery+RT+CT+Trastuzumab	2 (13%)
None	1 (6%)
Additional therapy	
ADT	2 (13%)
Disease recurrence	
No	6 (38%)
Local	1 (6%)
Distant	7 (44%)
Local and distant	2 (13%)

Clinical Feature	n (%) or mean (range)
Outcome	
Alive without disease	4 (25%)
Alive with disease	2 (13%)
Death from disease	8 (50%)
Death from other causes	2 (13%)

*At time of diagnosis.

RT, Radiotherapy; CT, chemotherapy (carboplatin in combination with paclitaxel or fluorouracil). ADT, androgen-deprivation therapy (bicalutamide and luprolide).